ELSEVIER

Journal of Organometallic Chemistry 549 (1997) 155–161

Journal of Organometallic Chemistry

Different coordination modes of 3-hydroxy-1,2,3-benzotriazin-4(3*H*)-one: Molecular structures of (μ-H)$Os_3(CO)_{10}$(μ_2-(2,3-η^2)-(O)NNNC$_7$H$_4$O) and (μ-H)$Ru_3(CO)_{10}$(μ_2-(1,2-η^2)-NNN(O)C$_7$H$_4$O)

Sudalaiandi Kumaresan [a], Kuang-Lieh Lu [a,*], Jui-Te Hung [a], Fang-Yuan Lee [a], Yuh-Sheng Wen [a], Jih Ru Hwu [a,b,*]

[a] *Institute of Chemistry, Academia Sinica, Taipei 11529, Taiwan, Republic of China*
[b] *Department of Chemistry, National Tsing Hua University, Hsinchu 30043, Taiwan, Republic of China*

Received 27 May 1997; received in revised form 27 June 1997

Abstract

Reaction of $Os_3(CO)_{10}(NCMe)_2$ with 3-hydroxy-1,2,3-benzotriazin-4(3*H*)-one (**1**) in CH_2Cl_2 gave the *N*-oxide complex (μ-H)$Os_3(CO)_{10}$(μ_2-(2,3-η^2)-(O)NNNC$_7$H$_4$O) (**2**). Following similar conditions, $Ru_3(CO)_{10}(NCMe)_2$ reacted with **1** to afford (μ-H)$Ru_3(CO)_{10}$(μ_2-(1,2-η^2)-NNN(O)C$_7$H$_4$O) (**3**). Results from single-crystal X-ray diffraction analyses for **2** and **3** revealed that ligand **1** exhibited different coordination modes towards triosmium and triruthenium clusters. Both structures show that the ligand coordinated axially at two metal centres of the triangular clusters. However, ligand **1** is bound to complex **2** in a μ_2-(2,3-η^2-*N-O*) coordination mode, whereas, it exhibits a μ_2-(1,2-η^2-*N-N'*) coordination mode in **3**. Complex **2** crystallized in the monoclinic space group $P2_1/n$ with a = 8.159(2) Å, b = 19.778(3) Å, c = 13.857(3) Å; β = 95.862(2)°; V = 2224.3(8) Å^3, Z = 4, R = 3.9%, R_w = 4.6%. Complex **3** crystallized in the triclinic space group $P\bar{1}$ with a = 8.496(2) Å, b = 14.523(2) Å, c = 18.445(1) Å; α = 85.801(9)°, β = 83.874(1)°, γ = 78.825(2)°; V = 2216.8(7) Å^3, Z = 4, R = 3.1%, R_w = 3.2%. © 1997 Elsevier Science S.A.

1. Introduction

N-Hydroxy derivatives of 2-aminofluorene, β-naphthylamine, and *p*-phenetidine are potent direct-acting mutagens [1,2]. For example, *N*-hydroxylaminopurines are mutagenic for many prokaryotic and eukaryotic species [3]. Recent reports indicate that *N*-arylhydroxamic acids and *N*-arylhydroxylamines can cause DNA strand scissions and gene damage: heterolytic fission of the N–O bond can generate nitrenium ions, which would interact with the nucleophilic sites on the DNA bases [4,5] (for DNA scission, also see Ref. [6]). In the course of our attempts to develop organometallic compounds as DNA cleaving agents, we have investigated the preparation of certain novel osmium *N*-oxide complexes from the reaction of triosmium clusters with 1-hydroxybenzotriazole, in which the *N*-hydroxyl ligand was converted to an *N*-oxide functional group and the ligand coordinated at the osmium clusters in a μ_2-(2,3-η^2-*N-N'*) coordination mode [7].

In this paper, we report the syntheses and molecular structures of (μ-H)$Os_3(CO)_{10}$(μ_2-(2,3-η^2)-(O)NNNC$_7$H$_4$O) (**2**) and (μ-H)$Ru_3(CO)_{10}$(μ_2-(1,2-η^2)-NNN(O)C$_7$H$_4$O) (**3**). These compounds were prepared by reaction of an *N*-hydroxyl derivative, 3-hydroxy-1,2,3-benzotriazin-4(3*H*)-one (**1**), with osmium and ruthenium clusters. Our study was prompted by the results that several ruthenium complexes [8] and 3-hydroxy-1,2,3-benzotriazin-4(3*H*)-one (**1**) [9] exhibit special biological properties. In addition, ligand **1** possesses a nucleus bearing a hydroxamic acid and a triazine moieties, which present fruitful chemistry [10–12]. We found that the coordination mode of the ligand **1** with the osmium cluster deviated from that of the ruthenium cluster.

* Corresponding author.

PII S0022-328X(97)00417-8

2. Results and discussion

2.1. Preparation of $(\mu\text{-}H)Os_3(CO)_{10}(\mu_2\text{-}(2,3\text{-}\eta^2)\text{-}(O)NNNC_7H_4O)$ (2)

We treated the 'lightly ligated' complex $Os_3(CO)_{10}(NCMe)_2$ with 3-hydroxy-1,2,3-benzotriazin-4(3*H*)-one (**1**) in CH_2Cl_2 at 0°C to give $(\mu\text{-}H)Os_3(CO)_{10}(\mu_2\text{-}(2,3\text{-}\eta^2)\text{-}(O)NNNC_7H_4O)$ (**2** Scheme 1). Its ^1H NMR spectrum showed a hydride signal at $\delta = -10.19$, which came from the proton of the hydroxyl group in the activated **1**. The FAB mass spectrum of **2** exhibited the molecular ion peak at m/z 1017 and peaks related to subsequent CO-loss fragments.

By use of the single-crystal X-ray diffraction method, we obtained solid evidence to support the structure of complex **2**. An ORTEP drawing of **2** is shown in Fig. 1. Its pertinent crystallographic data are given in Tables 1–3. This complex consisted of a triangular cluster of osmium atoms with distances 2.866(1) Å for Os(1)–Os(2), 2.883(1) Å for Os(1)–Os(3), and 2.876(1) Å for Os(2)–Os(3). Pseudo-octahedral geometry is observed around the Os atoms. The activated **1** coordinated axially at the Os(2) and the Os(3) atoms with a μ_2-(2,3-η^2-*N-O*) coordination mode. The bond angles of N(2)–Os(3)–C(8) and O(12)–Os(2)–C(5) were 178.2(7)° and 172.2(7)°, respectively. The five contiguous atoms, Os(2), Os(3), N(2), N(1), and O(12) were almost coplanar. This plane was nearly orthogonal to the plane defined by the three Os atoms. The torsion angles of Os(1)–Os(2)–Os(3)–N(2) and O(12)–Os(2)–Os(3)–Os(1) were 94.0(4)° and −97.9(3)°, respectively. The bridging hydride is expected to coordinate at the Os(2) and the Os(3) atoms although the bond distance of Os(2)–Os(3) was slightly shorter than that of Os(1)–Os(3).

A single bridging hydride ligand produces an elongation effect on metal–metal bond [13]. Nevertheless, when a μ_2-bridging ligand coexists with the bridging

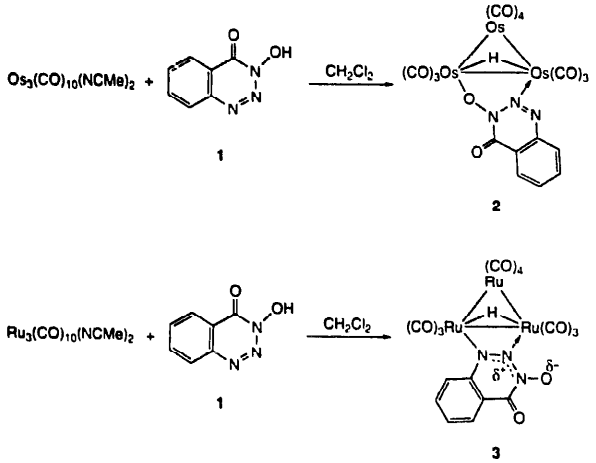

Scheme 1.

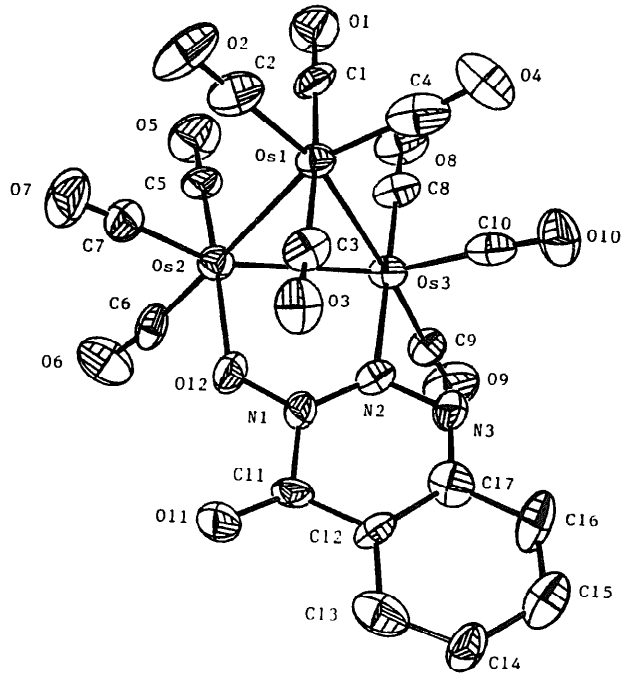

Fig. 1. ORTEP diagram of $(\mu\text{-}H)Os_3(CO)_{10}(\mu_2\text{-}(2,3\text{-}\eta^2)\text{-}(O)NNNC_7H_4O)$ (**2**).

Table 1
Crystal and Intensity Collection Data for $(\mu\text{-}H)Os_3(CO)_{10}(\mu_2\text{-}(2,3\text{-}\eta^2)\text{-}(O)NNNC_7H_4O)$ (**2**) and $(\mu\text{-}H)Ru_3(CO)_{10}(\mu_2\text{-}(1,2\text{-}\eta^2)\text{-}NNN(O)C_7H_4O)$ (**3**)

compound	**2**	**3**
formula	$C_{17}H_5N_3O_{12}Os_3$	$C_{17}H_5N_3O_{12}Ru_3$
fw	1013.84	746.45
space group	$P2_1/n$	$P\bar{1}$
a (Å)	8.1585(15)	8.4959(22)
b (Å)	19.778(3)	14.5233(23)
c (Å)	13.857(3)	18.4454(14)
α (deg)		85.801(9)
β (deg)	95.862(17)	83.874(13)
γ (deg)		78.825(17)
V (Å^3)	2224.3(8)	2216.8(7)
D_{calc} (mg m^{-3})	3.028	2.237
Z	4	4
crystal dimension (mm)	0.13×0.38×0.16	0.24×0.01×0.14
absorption coefficient μ(Mo Kα) (mm^{-1})	17.18	2.05
temperature	room temperature	room temperature
radiation	Mo Kα	Mo Kα
2θ (max)	45°	45°
scan type	$\theta/2\theta$	$\theta/2\theta$
total no. of reflection	2948	6257
no. of observed reflection $F_o > 2.0\sigma(F_o)$	2284	4004
observed variables	317	633
R	0.039	0.031
R_w	0.046	0.032
$\Delta(\rho)$ (e Å^{-3})	3.310, −1.620	0.490, −0.460
Δ/σ_{max}	0.017	0.026
GOF	2.32	1.45

Table 2
Atomic coordinates and isotropic thermal parameters (Å^2) for (μ-H)Os$_3$(CO)$_{10}$(μ_2-(2,3-η^2)-(O)NNNC$_7$H$_4$O) (2)

Atom	x	y	z	B_{iso}[a]
Os(1)	0.05100(9)	0.85692(4)	0.11228(5)	2.67(3)
Os(2)	0.19546(9)	0.81800(4)	−0.05939(5)	2.79(3)
Os(3)	0.28913(8)	0.74884(4)	0.12037(5)	2.61(3)
O(1)	0.3349(18)	0.9605(8)	0.1627(10)	5.1(7)
O(2)	−0.1773(19)	0.9728(8)	0.0437(13)	6.5(10)
O(3)	−0.2372(16)	0.7615(8)	0.0437(9)	4.3(7)
O(4)	−0.0297(19)	0.8548(9)	0.3238(11)	6.0(9)
O(5)	0.4571(18)	0.9257(8)	−0.0395(11)	5.8(8)
O(6)	0.3241(18)	0.7824(9)	−0.2511(11)	5.7(8)
O(7)	−0.0623(19)	0.9147(9)	−0.1592(11)	5.9(8)
O(8)	0.5678(16)	0.8420(7)	0.1916(11)	4.8(8)
O(9)	0.5288(18)	0.6323(8)	0.1185(12)	5.8(9)
O(10)	0.1938(17)	0.7179(8)	0.3229(10)	5.0(8)
O(11)	−0.1553(16)	0.6354(7)	−0.1486(9)	4.3(7)
O(12)	0.0377(15)	0.7330(6)	−0.0841(8)	3.4(6)
N(1)	0.0196(17)	0.6823(7)	−0.0251(10)	2.6(7)
N(2)	0.0964(17)	0.6791(8)	0.0642(10)	2.8(7)
N(3)	0.0680(18)	0.6318(8)	0.1269(10)	3.1(7)
C(1)	0.2308(25)	0.9189(10)	0.1416(14)	3.6(10)
C(2)	−0.0900(26)	0.9299(12)	0.0688(16)	4.5(11)
C(3)	−0.1226(24)	0.7966(11)	0.0706(14)	3.4(10)
C(4)	0.0013(23)	0.8541(11)	0.2407(18)	4.7(12)
C(5)	0.3532(25)	0.8856(10)	−0.0467(13)	3.5(10)
C(6)	0.2834(21)	0.7927(10)	−0.1747(14)	3.3(9)
C(7)	0.0302(27)	0.8805(11)	−0.1216(14)	3.8(10)
C(8)	0.4590(24)	0.8075(10)	0.1658(15)	3.8(10)
C(9)	0.4387(23)	0.6742(10)	0.1160(13)	3.2(9)
C(10)	0.2293(22)	0.7318(10)	0.2450(16)	3.6(10)
C(11)	−0.0981(21)	0.6302(9)	−0.0629(13)	2.8(8)
C(12)	−0.1314(21)	0.5800(9)	0.0059(13)	2.9(9)
C(13)	−0.2449(22)	0.5277(11)	−0.0183(14)	4.0(10)
C(14)	−0.2737(22)	0.4828(10)	0.0519(14)	3.6(9)
C(15)	−0.1928(25)	0.4854(11)	0.1471(16)	4.4(11)
C(16)	−0.0828(24)	0.5349(12)	0.1681(15)	4.4(11)
C(17)	−0.0487(20)	0.5845(11)	0.0989(13)	3.2(9)

[a] B_{iso} is the mean of the principal axes of the thermal ellipsoid.

Table 3
Selected bond distances and angles for (μ-H)Os$_3$(CO)$_{10}$(μ_2-(2,3-η^2)-(O)NNNC$_7$H$_4$O) (2)

Bond distances (Å)			
Os(1)–Os(2)	2.8659(11)	Os(1)–Os(3)	2.8831(11)
Os(2)–Os(3)	2.8760(12)	Os(2)–O(12)	2.124(12)
Os(3)–N(2)	2.174(14)	O(12)–N(1)	1.314(19)
N(1)–N(2)	1.331(20)	N(1)–C(11)	1.466(22)
N(2)–N(3)	1.314(21)	N(3)–C(17)	1.362(25)
C(11)–C(12)	1.42(3)	C(12)–C(17)	1.395(25)

Bond angles (deg)			
Os(2)–Os(1)–Os(3)	60.03(3)	Os(1)–Os(2)–Os(3)	60.28(3)
Os(1)–Os(2)–Os(12)	93.0(3)	Os(3)–Os(2)–O(12)	82.3(3)
O(12)–Os(2)–C(5)	172.2(7)	Os(1)–Os(3)–Os(2)	59.69(3)
Os(1)–Os(3)–N(2)	89.8(4)	Os(2)–Os(3)–N(2)	82.7(4)
N(2)–Os(3)–C(8)	178.2(7)	Os(2)–O(12)–N(1)	127.6(10)
O(12)–N(1)–N(2)	122.7(14)	O(12)–N(1)–C(11)	115.1(13)
N(2)–N(1)–C(11)	122.1(14)	Os(3)–N(2)–N(1)	124.0(11)
Os(3)–N(2)–N(3)	112.7(11)	N(1)–N(2)–N(3)	123.2(14)
N(2)–N(3)–C(17)	117.8(14)	O(11)–C(11)–N(1)	117.1(16)
O(11)–C(11)–C(12)	128.6(16)	N(1)–C(11)–C(12)	114.3(15)
C(11)–C(12)–C(13)	121.3(17)	C(11)–C(12)–C(17)	117.9(16)
N(3)–C(17)–C(12)	124.4(17)	Os(1)–Os(2)–C(7)	82.7(6)
Os(2)–Os(3)–C(9)	116.9(5)	Os(2)–Os(1)–C(2)	103.1(6)
Os(3)–Os(2)–C(6)	121.2(5)	Os(3)–Os(1)–C(4)	98.8(6)
Os(1)–Os(3)–C(10)	86.1(6)		

hydride, the doubly bridged metal–metal vector could be either longer or shorter than the nonbridged metal–metal bond [13]. The significantly large angles of Os(2)–Os(3)–C(9) [116.9(5)°] and Os(3)–Os(2)–C(6) [121.2(5)°] indicate that the bridging hydride introduced a 'pushing back' effect on the adjacent carbonyl ligands at the equatorial position [14]. This effect is clear by the observation of the other smaller Os–Os–C (equatorial) angles in **2** (∠Os(1)–Os(2)–C(7) = 82.7(6)°, ∠Os(2)–Os(1)–C(2) = 103.1(6)°, ∠Os(3)–Os(1)–C(4) = 98.8(6)°, ∠Os(1)–Os(3)–C(10) = 86.1(6)°). We observed 1.24(2) Å for the C(11)–O(11) bond length, which is close to the typical figure of a ketonic C=O [15]. The bond distance of N(1)–O(12) [1.31(2) Å] is in the normal range of the *N*-oxide moiety [15]. O(12) of the *N*-oxide coordinates at Os(2) but the polarity of the molecule was much less than that of the related *N*-oxide complexes [16].

2.2. Preparation of (μ-h)Ru$_3$(CO)$_{10}$(μ_2-(1,2-η^2)-NNN(O)C$_7$H$_4$O) (3)

We prepared Ru$_3$(CO)$_{10}$(NCMe)$_2$ by oxidation of Ru$_3$(CO)$_{12}$ with trimethylamine *N*-oxide in acetonitrile

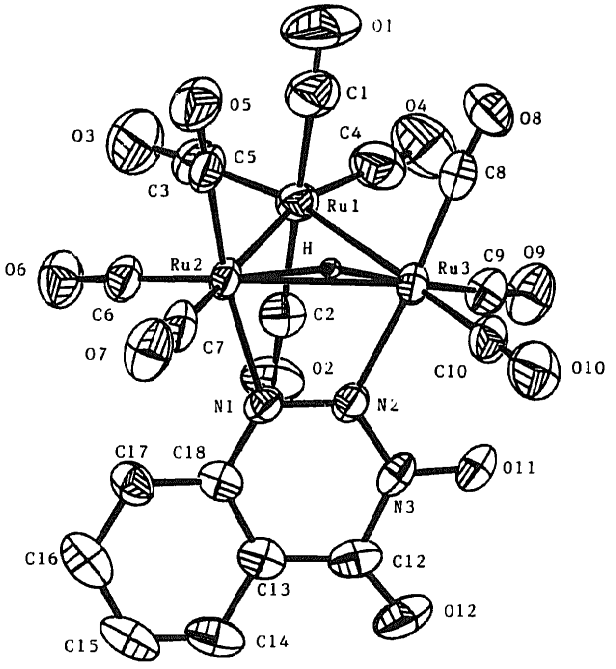

Fig. 2. ORTEP diagram of (μ-H)Ru$_3$(CO)$_{10}$(μ_2-(1,2-η^2)-NNN(O)C$_7$H$_4$O) (3).

Table 4
Atomic coordinates and isotropic thermal parameters (Å^2) for (μ-H)Ru$_3$(CO)$_{10}$(μ_2-(1,2-η^2)-NNN(O)C$_7$H$_4$O) (3)

Atom	x	y	z	B_{iso}[a]
Ru(1)	0.31608(9)	0.28413(5)	0.30315(4)	3.30(3)
Ru(2)	0.23959(8)	0.20570(4)	0.17760(4)	2.92(3)
Ru(3)	0.55861(8)	0.15502(5)	0.22671(4)	2.90(3
Ru(4)	0.18799(9)	0.81214(5)	0.40446(4)	4.03(4)
Ru(5)	0.12282(8)	0.70457(5)	0.29148(4)	2.98(3)
Ru(6)	0.41693(8)	0.65210(5)	0.35709(4)	3.01(3)
N(1)	0.4067(7)	0.2732(4)	0.1081(3)	2.8(3)
N(2)	0.5504(7)	0.2469(4)	0.1333(3)	2.8(3)
N(3)	0.6836(7)	0.2714(4)	0.0974(4)	3.3(3)
N(4)	0.3147(7)	0.7498(4)	0.2211(3)	2.7(3)
N(5)	0.4480(7)	0.7221(4)	0.2543(3)	2.8(3)
N(6)	0.5904(8)	0.7359(5)	0.2237(4)	3.8(4)
O(1)	0.2093(10)	0.1233(5)	0.4031(4)	8.3(5)
O(2)	0.4222(8)	0.4350(4)	0.1951(3)	5.2(4)
O(3)	0.0013(9)	0.4163(5)	0.3420(4)	8.3(5)
O(4)	0.4966(10)	0.3372(5)	0.4215(4)	8.0(5)
O(5)	0.0438(8)	0.0835(4)	0.2714(4)	6.6(4)
O(6)	−0.0287(7)	0.3790(4)	0.1781(4)	5.2(3)
O(7)	0.1454(7)	0.1156(4)	0.0499(4)	5.7(3)
O(8)	0.5497(8)	0.0164(4)	0.3561(3)	5.3(3)
O(9)	0.7849(7)	0.2481(4)	0.3002(4)	5.5(4)
O(10)	0.8228(8)	0.0158(4)	0.1455(4)	6.2(4)
O(11)	0.8156(7)	0.2391(4)	0.1224(3)	4.9(3)
O(12)	0.8085(7)	0.3516(4)	0.0058(3)	5.5(3)
O(21)	0.0177(12)	0.6931(6)	0.5183(4)	11.4(6)
O(22)	0.3432(8)	0.9258(4)	0.2796(4)	5.8(4)
O(23)	0.3703(12)	0.8779(6)	0.5195(5)	11.8(6)
O(24)	−0.1030(9)	0.9711(5)	0.4220(4)	8.5(5)
O(25)	−0.0890(8)	0.6034(5)	0.3965(4)	7.9(4)
O(26)	−0.1423(7)	0.8773(4)	0.2725(4)	5.8(3)
O(27)	0.0560(9)	0.5834(5)	0.1723(4)	6.5(4)
O(28)	0.3189(9)	0.5428(5)	0.4946(4)	6.9(4)
O(29)	0.6662(8)	0.4813(4)	0.3044(4)	6.8(4)
O(30)	0.6469(8)	0.7480(5)	0.4292(4)	6.8(4)
O(31)	0.7135(7)	0.7014(5)	0.2567(3)	5.7(4)
O(32)	0.7480(8)	0.8008(5)	0.1345(4)	6.2(4)
C(1)	0.2506(12)	0.1796(6)	0.3635(5)	5.3(5)
C(2)	0.3846(10)	0.3764(5)	0.2335(5)	3.6(4)
C(3)	0.1152(11)	0.3652(6)	0.3287(5)	4.9(5)
C(4)	0.4294(12)	0.3145(6)	0.3776(5)	5.1(5)
C(5)	0.1174(10)	0.1325(6)	0.2386(5)	4.4(5)
C(6)	0.0706(10)	0.3137(5)	0.1780(5)	3.7(4)
C(7)	0.1873(10)	0.1493(6)	0.0960(5)	3.9(5)
C(8)	0.5485(10)	0.0710(6)	0.3079(5)	3.7(4)
C(9)	0.7022(10)	0.2139(6)	0.2719(5)	3.9(4)
C(10)	0.7240(10)	0.0666(6)	0.1745(5)	4.0(4)
C(12)	0.6822(10)	0.3322(5)	0.0309(4)	3.6(4)
C(13)	0.5252(10)	0.3578(5)	0.0051(4)	3.2(4)
C(14)	0.5063(12)	0.4135(6)	−0.0607(5)	4.5(5)
C(15)	0.3591(13)	0.4362(6)	−0.0867(5)	5.2(5)
C(16)	0.2245(12)	0.4088(6)	−0.0462(5)	5.0(5)
C(17)	0.2405(10)	0.3527(6)	0.0172(4)	3.6(4)
C(18)	0.3928(10)	0.3267(5)	0.0446(4)	3.2(4)
C(21)	0.0856(14)	0.7355(8)	0.4752(5)	7.7(6)
C(22)	0.2877(11)	0.8821(6)	0.3252(5)	4.1(4)
C(23)	0.3043(14)	0.8539(7)	0.4777(6)	7.0(6)
C(24)	0.0008(12)	0.9119(7)	0.4151(5)	5.4(5)
C(25)	−0.0152(10)	0.6462(6)	0.3585(5)	4.8(5)
C(26)	−0.0435(10)	0.8132(6)	0.2773(5)	3.8(4)
C(27)	0.0827(10)	0.6308(6)	0.2130(5)	4.4(5)
C(28)	0.3551(11)	0.5868(6)	0.4438(5)	4.4(4)
C(29)	0.5743(10)	0.5443(6)	0.3226(5)	4.1(5)
C(30)	0.5523(11)	0.7123(6)	0.4023(5)	4.5(5)
C(32)	0.6135(10)	0.7894(6)	0.1566(5)	4.0(4)
C(33)	0.4686(11)	0.8206(5)	0.1231(4)	4.0(4)
C(34)	0.4710(13)	0.8735(6)	0.0561(5)	5.3(5)
C(35)	0.3360(14)	0.9014(6)	0.0225(5)	5.5(6)
C(36)	0.1895(13)	0.8767(6)	0.0529(5)	5.4(5)
C(37)	0.1855(11)	0.8266(6)	0.1170(5)	4.0(5)
C(38)	0.3218(10)	0.7981(5)	0.1548(4)	3.2(4)
H-1	0.404	0.116	0.194	3.8(17)
H-2	0.273	0.609	0.312	4.4(18)

[a] B_{iso} is the mean of the principal axes of the thermal ellipsoid.

[17]. Treatment of $Ru_3(CO)_{10}(NCMe)_2$ with **1** in CH_2Cl_2 at −50 °C afforded the *N*-oxide complex (μ-H)Ru$_3$(CO)$_{10}$(μ_2-(1,2-η^2)-NNN(O)C$_7$H$_4$O) (**3**) in 11% yield and traces of an unidentified compound **3a**.

The ^{1}H NMR spectrum of **3** showed a singlet at $\delta = -13.54$, which is assigned to a bridging hydride. The resonances attributed to the aromatic protons of the ligand appeared in the range δ 7.42–8.26. The ^{13}C NMR spectrum exhibited 11 resonances in the region from δ 153.0–203.9, which can be attributed to the 11 carbonyl carbons. The FAB mass spectrum of **3** showed the molecular ion peak at *m/z* 749 and peaks resulting from the subsequent CO-loss fragments. The ^{1}H NMR spectrum of complex **3a** showed a singlet at $\delta = -13.07$ attributed to a bridging hydride and multiplets at δ 7.48–8.17 due to aromatic protons. However, the structure of **3a** has not been fully characterized. An ORTEP diagram of (μ-H)Ru$_3$(CO)$_{10}$(μ_2-(1,2-η^2)-NNN(O)C$_7$H$_4$O) (**3**) from X-ray analysis is shown in Fig. 2; relevant crystallographic details are listed in Tables 4 and 5. Two crystallographically independent molecules were present within the asymmetric unit. The three Ru atoms defined an isosceles triangle; the Ru(2) and the Ru(3) atoms were doubly bridged by a hydride and two contiguous nitrogen atoms N(1) and N(2). The activated 3-hydroxy-1,2,3-benzotriazin-4(3*H*)-one (**1**) coordinated axially at the Ru(2) and the Ru(3) atoms with a μ_2-(1,2-η^2-*N*-*N'*) coordination mode. The plane defined by the Ru(2), Ru(3), N(2), and N(1) atoms was found nearly orthogonal to that defined by the three Ru atoms; such a geometry is similar to that in the structures of both **2** and the related complex (μ-H)Os$_3$(CO)$_{10}$(μ_2-(2,3-η^2)-NNN(O)C$_6$H$_4$) [7]. The doubly bridged Ru(2)–Ru(3) vector [2.892(1) Å] in **3** was slightly longer than the nonbridged bonds [Ru(1)–Ru(2) = 2.842(1) Å and Ru(1)–Ru(3) = 2.832(1) Å]. The bridging hydride, which was observed crystallographically, coordinates between Ru(2) and Ru(3) in accord with the elongation of Ru(2)–Ru(3) bond and presented a 'pushing back' effect on the adjacent carbonyl ligands with large angles of Ru(3)–Ru(2)–C(7)

Table 5
Selected bond distances and angles for (μ-H)$Ru_3(CO)_{10}$(μ_2-(1,2-η^2)-NNN(O)C_7H_4O) (3)

Bond distances (Å)			
Ru(1)–Ru(2)	2.8420(11)	Ru(1)–Ru(3)	2.8318(11)
Ru(2)–Ru(3)	2.8916(12)	Ru(2)–N(1)	2.142(6)
Ru(3)–N(2)	2.099(6)	N(1)–N(2)	1.329(8)
N(1)–C(18)	1.361(9)	N(2)–N(3)	1.345(8)
N(3)–O(11)	1.251(8)	N(3)–C(12)	1.457(10)
C(12)–C(13)	1.436(12)	C(13)–C(18)	1.405(11)
Bond angles (deg)			
Ru(2)–Ru(1)–Ru(3)	61.28(3)	Ru(1)–Ru(2)–Ru(3)	59.19(3)
Ru(1)–Ru(2)–N(1)	91.60(17)	Ru(3)–Ru(2)–N(1)	69.39(16)
N(1)–Ru(2)–C(5)	172.0(3)	Ru(1)–Ru(3)–Ru(2)	59.53(3)
Ru(1)–Ru(3)–N(2)	90.71(17)	Ru(2)–Ru(3)–N(2)	67.27(16)
N(2)–Ru(3)–C(8)	174.9(3)	Ru(2)–N(1)–N(2)	107.6(4)
Ru(2)–N(1)–C(18)	132.5(5)	N(2)–N(1)–C(18)	119.6(6)
Ru(3)–N(2)–N(1)	115.7(4)	Ru(3)–N(2)–N(3)	122.4(5)
N(1)–N(2)–N(3)	121.7(6)	N(2)–N(3)–O(11)	117.7(6)
N(2)–N(3)–C(12)	123.6(6)	O(11)–N(3)–C(12)	118.7(6)
N(3)–C(12)–O(12)	117.0(8)	N(3)–C(12)–C(13)	112.8(7)
O(12)–C(12)–C(13)	130.2(8)	C(12)–C(13)–C(18)	120.0(7)
Ru(3)–Ru(2)–C(7)	120.5(2)	Ru(2)–Ru(1)–C(3)	100.0(3)
Ru(2)–Ru(3)–C(10)	120.4(3)	Ru(1)–Ru(3)–C(9)	83.9(3)
Ru(1)–Ru(2)–C(6)	83.0(3)	Ru(3)–Ru(1)–C(4)	101.1(3)

[120.5(2)°] and Ru(2)–Ru(3)–C(10) [120.4(3)°]. This is collaborated by the existence of the other smaller Ru–Ru–C (equatorial) angles. The C(12)–O(12) bond length of 1.20(1) Å indicates a double bond character, which is similar to that found in **2**. The bond distance of N(3)–O(11) [1.251(8) Å] is slightly shorter than that in normal *N*-oxides [15]. Our X-ray results indicate that the N(1)–N(2) [1.329(8) Å] and the N(2)–N(3) [1.345(8) Å] bonds bore partial double bond character.

It is of interest to compare the coordination modes of the ligand **1** in triosmium and triruthenium clusters. The molecular structures of **2** and **3** reveal that the activated ligand coordinated axially at two metal centres in both triangular clusters. The significant difference is that **1** exhibits a μ_2-(2,3-η^2-*N-O*) coordination mode toward complex **2**, whereas a μ_2-(1,2-η^2-*N-N'*) coordination mode in **3**. Furthermore, we have reported the synthesis of a related osmium *N*-oxide complex (μ-H)$Os_3(CO)_{10}$(μ_2-(2,3-η^2)-NNN(O)C_6H_4) from the reaction of triosmium clusters with 1-hydroxybenzotriazole [7], in which the *N*-oxide functional group coordinated at the osmium clusters in a μ_2-(2,3-η^2-*N-N'*) coordination mode. It is suggested that the carbonyl in 3-hydroxy-1,2,3-benzotriazin-4(3*H*)-one (**1**) plays a role in mediating the reactivity of the ligand toward trimetal clusters. First, the conjugated carbonyl group might decrease effectively the nucleophilicity of the N^1 atom in **1**. Second, the carbonyl may stabilize the adjacent hydroxyl group by forming an intramolecular hydrogen bonding [10] to build a five-membered ring and diminish the dissociation of the proton appreciably. As a consequence, the nucleophilic attack by the N^1 atom of the ligand might be hindered. Instead, oxidative addition of the hydroxyl group of **1** to the $Os_3(CO)_{10}(NCMe)$ moiety, which is the reaction intermediate via a dissociation of NCMe group from $Os_3(CO)_{10}(NCMe)_2$ [18,19], may occur to produce complex **2** with a special μ_2-(2,3-η^2-*N-O*) coordination mode. From the complex reaction mixture of $Ru_3(CO)_{10}(NCMe)_2$ with ligand **1**, compounds **3**, with a μ_2-(1,2-η^2-*N-N'*) coordination mode, and **3a** could be isolated albeit in a low yield.

In conclusion, the bidentate ligand 3-hydroxy-1,2,3-benzotriazin-4(3*H*)-one (**1**) chelated with a triosmium cluster through its =N–N–O moiety to form a five-membered ring complex. This ligand, however, coordinated to the ruthenium centres in the triruthenium cluster (μ-H)$Ru_3(CO)_{10}$(μ_2-(1,2-η^2)-NNN(O)C_7H_4O) (**3**) through its –N=N– moiety to form a four-membered ring complex. Acting as a ligand, the multifunctional compound (**1**) possessed different coordination modes in metal clusters. Performance of biological tests on its metal complexes is in due course.

3. Experimental section

3.1. General data

Reagents were purchased from commercial sources and were used as received. All manipulations, except for thin-layer chromatography (TLC), were performed under a nitrogen atmosphere by use of standard Schlenk techniques. Solvents were dried by stirring over Na/benzophenone (tetrahydrofuran and ether) or CaH_2 (hexanes and CH_2Cl_2) and were freshly distilled before use. IR spectra were recorded on a Perkin-Elmer 882 infrared spectrophotometer. NMR spectra were obtained on a Brucker MSL-200, an AC-200, or an AMX-500 FT-NMR spectrometer. Mass spectra were recorded on a VG 70-250S mass spectrometer. Elemental analyses were performed by use of a Perkin-Elmer 2400 CHN elemental analyzer.

3.2. Synthesis of (μ-H)$Os_3(CO)_{10}$(μ_2-(2,3-η^2)-(O)NNNC_7H_4O) (2)

A solution of $Os_3(CO)_{12}$ (201.0 mg, 0.222 mmol) in CH_2Cl_2 (150 ml) and CH_3CN (3.0 ml) was treated with a solution of Me_3NO (36.0 mg, 0.480 mmol) in CH_2Cl_2 (5.0 ml). The mixture was stirred at room temperature for 1 h and filtered through a short pad of silica gel. Removal of the solvent under reduced pressure afforded a yellow residue $Os_3(CO)_{10}(NCMe)_2$, which was redissolved in CH_2Cl_2 (150 ml) precooled to −50°C. To the resultant solution was added a solution of 3-hydroxy-

1,2,3-benzotriazin-4(3*H*)-one (**1**, 36.0 mg, 0.221 mmol) in dry acetone (5.0 ml) at −50 °C. This mixture was stirred at 20–25 °C for 20 h. Then the solvent was removed under reduced pressure and the residue was purified on a silica gel TLC plate (2-mm thickness) with CH_2Cl_2 as the eluent to afford **2** as a red-orange powder (86.0 mg, 0.0846 mmol) in 38% yield. Anal. calcd. for $C_{17}H_5N_3O_{12}Os_3$: C, 20.14; H, 0.50; N, 4.14. Found: C, 20.78; H, 0.50; N, 3.90. IR (CH_2Cl_2): ν(CO) 2128(w), 2115(m), 2080(s), 2065(s), 2031(s), 2017(s), 1985(sh), 1708(w) cm^{-1}. ^1H NMR ($CDCl_3$): δ 8.10 (d, J = 7.9 Hz, 1H, aromatic), 7.72–7.85 (m, 2H, aromatic), 7.51–7.58 (m, 1H, aromatic), −10.19 (s, 1H, Os–H–Os). ^{13}C NMR ($CDCl_3$/DMSO-d_6): δ 181.1, 180.9, 175.1, 175.0, 174.1, 173.9, 173.7, 173.4, 173.2, 172.7, 153.1 (CO), 144.8, 133.8, 131.9, 129.5, 124.5, 117.1 (aromatic). MS (FAB, ^{192}Os): m/z 1017 (M^+, 89%), 989 (M^+-CO, 35%), 961 (M^+-2CO, 48%), 933 (M^+-3CO, 52%), 905 (M^+-4CO, 27%), 877 (M^+-5CO, 23%), 849 (M^+ - 6CO, 22%), 821 (M^+ - 7CO, 22%), 793 (M^+ - 8CO, 20%), 765 (M^+ - 9CO, 17%).

3.3. Preparation of (μ-H)$Ru_3(CO)_{10}$(μ_2-(1,2-η^2)-NNN(O)C_7H_4O) (3)

To a solution of $Ru_3(CO)_{12}$ (200.3 mg, 0.313 mmol) in CH_2Cl_2 (150 ml) and CH_3CN (10 ml) at −70 °C was added Me_3NO (60.2 mg, 0.803 mmol) in CH_3CN (5.0 ml) dropwise. After the solution was stirred at −70 °C for 10 min, it was warmed to room temperature for 30 min. The mixture was filtered through a short column of silica gel. The solvent was removed under reduced pressure and the resultant solid $Ru_3(CO)_{10}(NCMe)_2$ [17] was redissolved in CH_2Cl_2 (200 ml) precooled to −50 °C. To this solution was cannulated 3-hydroxy-1,2,3-benzotriazin-4(3*H*)-one (**1**, 51.4 mg, 0.315 mmol) in dry acetone (6.0 ml) slowly. After the mixture was stirred at ambient temperature for 2.0 h, the solvent was evaporated under reduced pressure and the remaining dark brown solid was purified on a silica gel TLC plate (2-mm thickness). $Ru_3(CO)_{12}$ was eluted with hexane (60.0 mg). A violet band followed by an orange band were eluted with a mixture of CH_2Cl_2 and THF as the eluent (97:3). Complex **3a** was obtained as a dark red powder (3.0 mg) from the violet band. IR (CH_2Cl_2): ν(CO) 2101(w), 2060(s), 2028(s), 2008(sh), 1969(w) cm^{-1}. ^1H NMR ($CDCl_3$): δ 8.15 (d, J = 8.3 Hz, 1H, aromatic), 7.85 (d, J = 8.4 Hz, 1H, aromatic), 7.64–7.48 (m, 2H, aromatic), −13.07 (s, 1H, bridging hydride). Complex **3** was obtained as a red-orange powder (19.0 mg, 0.0253 mmol) from the orange band in 11% yield based on the consumed $Ru_3(CO)_{12}$. Anal. calcd. for $C_{17}H_5N_3O_{12}Ru_3$: C, 27.25; H, 0.67; N, 5.61. Found: C 27.82; H, 1.37; N, 5.34. IR (CH_2Cl_2): ν(CO) 2112(m), 2080(s), 2066(s), 2038(m), 2024(s) cm^{-1}. ^1H NMR ($CDCl_3$): δ 8.26 (d, J = 8.0 Hz, 1H, aromatic), 7.86 (overlapping dd, J = 7.6 Hz, 1H, aromatic), 7.42–7.52 (m, 2H, aromatic), −13.54 (s, 1H, Ru–H–Ru). ^{13}C NMR ($CDCl_3$): δ 203.9, 203.5, 200.3, 199.2, 194.1, 189.8, 189.6, 187.7, 184.5, 183.5, 153.0 (CO), 145.3, 134.9, 127.7, 127.2, 120.7, 115.4 (aromatic). MS (FAB, ^{102}Ru): m/z 749 (M^+, 56%), 721 (M^+-CO, 67%), 693 (M^+ - 2 CO, 24%), 665 (M^+ - 3CO, 33%), 637 (M^+ - 4CO, 100%), 609 (M^+ - 5CO, 46%), 581 (M^+ - 6CO, 41%), 553 (M^+ - 7CO, 52%), 525 (M^+ - 8CO, 63%), 497 (M^+ - 9CO, 46%), 469 (M^+ - 10CO, 41%). Some decomposed products remained on the base line.

3.4. Crystallographic structure studies.

Crystals of **2** and **3** suitable for X-ray diffraction studies were grown by vapour diffusion of Et_2O into a $CHCl_3$ solution of the compounds at −5 °C. Specimens of suitable quality were mounted in thin-walled glass capillaries and used for measurement of precise cell constants and intensity data collection. All diffraction measurements were made on an Enraf-Nonius CAD-4 diffractometer by use of graphite–monochromatized Mo Kα radiation (λ = 0.70930 Å) with θ–2θ scan mode. Unit cells were determined and refined by use of 25 randomly selected reflections obtained with the aid of the CAD-4 automatic search, center, index and least-squares routines. Anomalous dispersion corrections were applied to all non-hydrogen atoms. Lorentz/polarization (L_p) and empirical absorption corrections on the basis of three azimuthal scans were applied to the data for each structure. Compound **2** crystallized in the monoclinic crystal system and complex **3** crystallized in the triclinic crystal system. The systematic absences in the diffraction data of **2** unambiguously established the space group as $P2_{1/n}$. The centrosymmetric space group was initially assumed and later confirmed by the results of refinement for **3**. The structures were solved by the Patterson method. All remaining non-hydrogen atoms were located from the difference Fourier map, and they were included in the final refinement cycle and refined by full-matrix least squares. The hydride peak in **3** was located and refined. All the data processing was carried out on a Microvax 3600 by use of the NRCC SDP program [20].

For **2** and **3**, Tables 1–5 offer crystal and intensity collection data, atomic coordinates, anisotropic thermal parameters, and bond lengths and angles.

Acknowledgements

Financial support from the National Science Council of the Republic of China is gratefully acknowledged.

References

[1] J. McCann, I. Choi, E. Yamasaki, B.N. Ames, Proc. Natl. Acad. Sci. U.S.A. 72 (1975) 5135.

[2] T. Nohmi, K. Yoshikawa, M. Nakadate, M. Ishidate Jr., Biochem. Biophys. Res. Commun. 110 (1983) 746.

[3] M. McCartney, E.C. McCoy, H.S. Rosenkranz, A. Giner-Sorolla, Mutat. Res. 144 (1985) 231, references cited therein.

[4] S. Hashimoto, R. Yamashita, Y. Nakamura, Chem. Lett. (1992) 1639.

[5] M. Novak, M.J. Kahley, E. Eiger, J.S. Helmick, H.E. Peters, J. Am. Chem. Soc. 115 (1993) 9453, references cited therein.

[6] J.R. Hwu, S.C. Tsay, B.L. Chen, H.V. Patel, C.T. Chou, J. Chem. Soc., Chem. Commun. (1994) 1427.

[7] K.L. Lu, S. Kumaresan, Y.S. Wen, J.R. Hwu, Organometallics 13 (1994) 3170.

[8] C.A. McAuliffe, H.I. Sharma, N.D. Tinker, F.R. Hartley, in: F.R. Hartley (Ed.), Chemistry of the Platinum Group Metals: Recent Developments, Elsevier, New York, 1991, pp. 585–586.

[9] H. Neunhoffer, P.F. Wiley, Chem. Heterocycl. Compound 33 (1978) 165.

[10] T.P. Ahern, T. Navratil, K. Vaughan, Can. J. Chem. 55 (1977) 630.

[11] W. König, R. Geiger, Chem. Ber. 103 (1970) 2034.

[12] T.P. Ahern, T. Navratil, K. Vaughan, Tetrahedron Lett. 46 (1973) 4547.

[13] M.R. Churchill, R.A. Lashewycz, Inorg. Chem. 18 (1979) 1926.

[14] M.R. Churchill, B.G. DeBoer, Inorg. Chem. 16 (1977) 878.

[15] F.H. Allen, O. Kennard, D.G. Watson, L. Brammer, A.G. Orpen, R. Taylor, J. Chem. Soc., Perkin Trans. 2 (1987) S1.

[16] J.T. Hung, S. Kumaresan, L.C. Lin, Y.S. Wen, L.K. Liu, K.L. Lu, J.R. Hwu, Organometallics 15 (1996) 5605.

[17] G.A. Foulds, B.F.G. Johnson, J. Lewis, J. Organomet. Chem. 296 (1985) 147.

[18] K.L. Lu, M.L. Chung, P.Y. Lu, H.M. Gau, F.E. Hong, Y.S. Wen, Organometallics 13 (1994) 3177.

[19] A.J. Poë, in: M. Moskovits (Ed.), Metal Cluster, Wiley- Interscience, New York, 1986.

[20] E.J. Gabe, F.L. Lee, Y. Le Page, in: G.M. Sheldrick, C. Krüger, R. Goddard (Eds.), Crystallographic Computing 3: Data Collection, Structure Determination, Proteins, and Databases, Clarendon Press, Oxford, 1985, pp. 167–174.